FEBS Letters 574 (2004) 126–130 FEBS 28758

The trimeric organisation of photosystem I is not necessary for the iron-stress induced CP43′ protein to functionally associate with this reaction centre

Caroline L. Aspinwall[a,1], James Duncan[b,1], Thomas Bibby[b], Conrad W. Mullineaux[a], James Barber[b,*]

[a] *Department of Biology, University College London, Darwin Building, Gower Street, London WC1E 6BT, UK*
[b] *Wolfson Laboratories, Biochemistry Building, Department of Biological Sciences, Imperial College London, South Kensington Campus, London SW7 2AZ, UK*

Received 26 June 2004; revised 15 July 2004; accepted 12 August 2004

Available online 21 August 2004

Edited by Vladimir Skulachev

Abstract A mutant of *Synechocystis* PCC 6803 lacking the PsaL subunit of photosystem I (PSI) has been grown in iron-deficient media to induce the expression of the *isi*A gene, which encodes the chlorophyll *a*-binding protein CP43′. The purpose of this was to establish whether or not the formation of an 18-mer CP43′-PSI supercomplex reported for wild type *Synechocystis* cells [Nature 412 (2001) 743–745] was dependent on the trimeric conformation of the cyanobacterial PSI reaction centre. Structural characterisation by electron microscopy and single particle image analysis has revealed that the PsaL-mutant does not form trimers of PSI. However, despite this, CP43′ was found to associate with the PSI monomer. The PSI monomer bound six or seven copies of CP43′ along one edge of the PSI monomer and can be compared with one segment of the trimeric 18-mer CP43′-PSI supercomplex. We therefore conclude that the trimeric nature of cyanobacterial PSI is not required for the assembly of the CP43′ antenna system under iron-deficient conditions.

Keywords: Photosynthesis; Photosystem I; Electron microscopy; IsiA; CP43′; Cyanobacterium

1. Introduction

In cyanobacteria, the photosystem I (PSI) reaction centre is trimeric. Using deletion mutagenesis, Chitnis and Chitnis [1] showed that the PsaL subunit was required for maintaining this oligomeric organisation. Recently, the structure of this trimer, isolated from the thermophilic cyanobacteria *Thermosynechococcus elongatus*, has been determined to be 2.5 Å by X-ray crystallography [2]. This structure identified the location of the PsaL protein within the trimerisation domain in agreement with the conclusions of Chitnis and Chitnis [1]. Moreover, the X-ray structure showed that PsaL, a three-transmembrane helical protein, binds three chlorophyll *a* molecules that are believed to facilitate energy transfer between the three monomers in the reaction centre complex.

The question arises as to the functional significance of the trimeric structure of PSI in cyanobacteria. A possible answer to this question came from the recent discovery that under conditions of iron deficiency a light harvesting antenna associates with PSI. 18 subunits of the chlorophyll *a*-binding CP43′ protein form a ring around the PSI trimer [3–6]. CP43′ is a photosystem II (PSII)-like protein, encoded by the iron-stress induced *isi*A gene and increases the light harvesting capacity of PSI by almost 100%, as indicated by spectroscopic analyses [7,8]. It therefore seems to be possible that the trimeric conformation of the cyanobacterial PSI reaction centre is required for the formation of the 18-mer CP43′ antenna ring. In order to test this hypothesis, we have explored the effect of iron deficiency on a PsaL-minus (PsaL$^-$) mutant of *Synechocystis* sp. PCC 6803. To simplify the isolation of possible complexes of CP43′ with monomeric PSI, we constructed the PsaL deletion in a PSII-free mutant background.

2. Materials and methods

2.1. Construction of the PsaL$^-$ mutant

The *Synechocystis psa*L gene was PCR amplified from genomic DNA and cloned into the multiple cloning site of pBluescript SK+. *Hin*cII digestion of plasmid pUC4K [9] gave a DNA fragment containing an aminoglycoside 3′-phosphotransferase gene, which confers kanamycin resistance. This was inserted at a unique restriction site in the cloned *psa*L gene. The resulting construct, containing disrupted *psa*L, was transformed into cells of a PSII-minus strain of *Synechocystis* PCC 6803. This strain was a gift from Wim Vermaas (Arizona State University). The cells are completely deficient in PSII due to insertional inactivation of the *psb*D$_1$, *psb*C and *psb*D$_2$ genes with chloramphenicol and spectinomycin resistance cassettes [10]. Transformants were selected on BG11 agar containing 50 μg ml^{-1} kanamycin as well as 25 μg ml^{-1} chloramphenicol and 5 mM glucose. After repeated rounds of single colony selection to allow segregation, PCR confirmed that only disrupted copies of the *psa*L gene remained. The transformant is a null mutant for *psb*D$_1$, *psb*D$_2$, *psb*C and *psa*L, but will be referred to as PsaL$^-$ for the sake of simplicity.

2.2. Growth conditions

Synechocystis sp. PCC 6803 cells (wild type with His-tag [3,4] and PsaL$^-$) were grown photoheterotrophically in mineral medium BG11

* Corresponding author. Fax: +44-207-594-5267.
E-mail address: j.barber@imperial.ac.uk (J. Barber).

[1] Equal contributors to the research.

Abbreviations: PSII, photosystem II; PSI, photosystem I; EM, electron microscopy; DM, *n*-dodecyl-β-D-maltoside

0014-5793/$22.00 © 2004 Published by Elsevier B.V. on behalf of the Federation of European Biochemical Societies.
doi:10.1016/j.febslet.2004.08.016

supplemented with glucose (5 mM) at 30 °C and 10 μE m^{-2} s^{-1} illumination. The medium for PsaL$^-$ cells also contained kanamycin (50 μg ml^{-1}) and chloramphenicol (25 μg ml^{-1}). Iron-stressed cultures were obtained by growing cells in the same BG11 medium but lacking iron-containing compounds. Cultures were harvested after 4 days and in the case of iron-starved cultures, the cells had a characteristic blue shift in their long wavelength absorption band of about 7 nm compared with cells grown normally.

Thylakoid membranes were isolated using a procedure reported previously [3,4]. The isolated thylakoids (1 mg chl ml^{-1}) were solubilised with 1% *n*-dodecyl-β-D-maltoside (DM) at 4 °C for 10 min and centrifuged at 45 000 rpm using a Beckman Ti70 rotor. The solubilised fractions were layered on the top of a continuous sucrose gradient prepared according to the freeze–thaw method given in Hankamer et al. [11] and subjected to 12 h of centrifugation at 32 000 rpm using a Beckman SW40 rotor.

2.3. Biochemical characterisation

Sodium dodecyl sulfate (SDS)–polyacrylamide gel electrophoresis (PAGE) was performed as reported previously [3,4]. Optical absorption spectra were measured at room temperature using a Shimadzu MPS 2000 spectrometer (for isolated particles) or an Aminco DW2000 spectrometer (for cell cultures). Steady-state fluorescence spectra were obtained using a Perkin–Elmer LS50 at 77 K and measured with an excitation wavelength of 440 nm.

2.4. Electron microscopy and image processing

Samples were negatively stained with 2% uranyl acetate on glow discharged carbon evaporated grids and imaged using a Philips CM 100 electron microscope at 80 kV. The magnification was calibrated as being 51 500×, and electron micrographs were taken for each preparation and subsequently calculated to have the first minima of their contrast transfer functions to be in the range 17–25 Å. Electron micrographs were digitised using a Leafscan 45 densitometer set at a step size of 10 μm. Single particle data sets were obtained by interactively selecting all possible particles from the micrographs. All subsequent processing was performed within the IMAGIC-5 software environment [12,13]. The single particle images were coarsened by a factor of 2 resulting in a sampling frequency of 3.88 Å per pixel on the specimen scale. Reference free alignment coupled with multi-variate statistical analysis [14] was used to classify each data set in order to identify initial class averages. These were then used for iterative refinement, resulting in the improved class averages.

2.5. Modelling

Co-ordinate data sets were obtained from the RCSB Data bank (www.rcsb.org) under the entry codes for 1JB0.pdb (PSI 2.5 Å structure [2]) and 1S5L.pdb (PSII 3.5 Å structure [15]). These structural models were visualised using the program Swiss-PDB viewer (Glaxo-Wellcome Experimental Research) [16] and overlaid at the same scale onto the calculated single particle projection maps. The carbon-α backbone for the transmembrane helices of the CP43 subunit was extracted from the 1S5L.pdb co-ordinates and modelled into each CP43′ subunit.

3. Results

The *Synechocystis* sp. PCC 6803 PsaL$^-$ mutant was grown in BG11 media and iron-free BG11 media supplemented with glucose [3,4]. Room-temperature absorption spectra for cells are shown in Fig. 1(a), where it can be seen that iron deprivation resulted in a significant blue shift in the long wavelength absorption maximum. This well characterised response is due to the expression of the *isi*A gene resulting in the accumulation of CP43′ in the membrane. Isolated thylakoid membranes from the PsaL$^-$ mutant were solubilised using β-DM and subjected to sucrose density centrifugation as were control membranes from wild type *Synechocystis*. Fig. 1(b) shows the resulting profiles. Each band was subjected to absorption and fluorescence spectroscopy, SDS–PAGE analyses and negative stain electron microscopy (EM). In all cases, band 1 corresponded to monomers of PSI. The lowest fraction, band 3, was only found with the wild-type cells, grown in the presence of

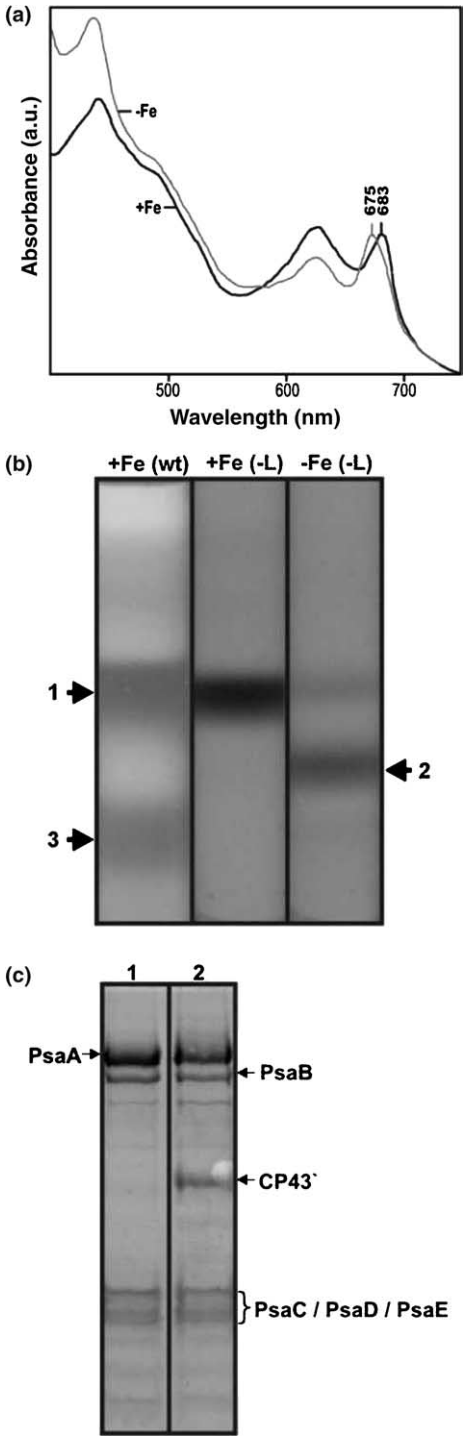

Fig. 1. (a) The room temperature absorption spectra of cells of a PSII-deficient PsaL$^-$ mutant of *Synechocystis* PCC 6803 grown in the presence (dark line, +Fe) or absence (grey line, −Fe) of iron. (b) Sucrose density gradients derived from centrifugation of solubilised PSI of wild-type and PSII-deficient PsaL$^-$ cells grown in the presence (+Fe) and absence (−Fe) of iron. (c) SDS–PAGE of Bands 1 and 2 from PSII-deficient PsaL$^-$ mutant cells grown in the presence (+Fe) and absence (−Fe) of iron.

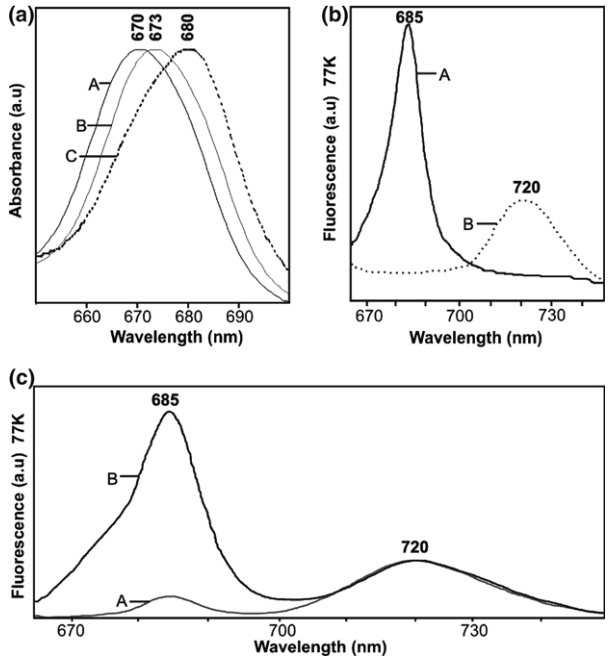

Fig. 2. (a) Room temperature absorption spectra of CP43′ isolated from wild type *Synechocystis* cells grown under low-iron conditions (dark line, A); band 2 (CP43′–PSI) defined in Fig. 1(b) (grey line, B) and band 1 (PSI monomers) defined in Fig. 1(b) (dotted line, C) having long wavelength absorption maxima at 670, 673 and 680 nm, respectively. (b) Fluorescence emission measured at 77 K for band 2 of Fig. 1(b) before (grey line, A) and after (dark line, B) addition of 0.1% Triton to the sample. (c) Fluorescence emission at 77 K from isolated CP43′ from *Synechocystis* cells grown under low iron conditions (dark line, A) and PSI monomers (band 1) (dotted line, B).

iron, and corresponded to PSI trimers. Band 2 was induced only in the PsaL$^-$ mutant under iron deficiency and SDS–PAGE (Fig. 1(c)) identified a protein corresponding to CP43′ as well as proteins of PSI, indicative of a CP43′–PSI supercomplex.

As seen in Fig. 2(a), the long wavelength absorption maximum of this supercomplex (band 2) was at 673 nm, which is positioned between the corresponding maxima of CP43′ (670 nm) and the PSI monomer (680 nm). This absorption maximum for band 2 is similar to that recorded for the 18-mer CP43′–PSI supercomplex [3,4]. The 77-K fluorescence was similar to that from the PSI monomers as shown in Fig. 2(b), except for some additional emission peaking at 685 nm. This short wavelength fluorescence is emitted from CP43′ as shown by comparison with the spectrum obtained using free CP43′ isolated from iron-deficient cells.

In order to explore the degree of functional linkage of CP43′ with PSI, we treated the band 2 sample with 0.1% Triton X-100 [4]. As recorded in Fig. 2(b), the 77 K spectra show that this detergent treatment results in a large increase of the relative emission at short wavelengths in a way similar to that observed when the 18-mer CP43′–PSI complex was subjected to the same detergent disruption [4].

The protein analysis of band 2, its position in the sucrose density gradient and the relatively low level of fluorescence emission from CP43′ in this fraction suggest that it contains a CP43′–PSI supercomplex. Indeed, HPLC size exclusion chromatography estimated that its molecular mass was approximately 640 kDa compared with 350 kDa for the PSI monomer. In order to investigate this possibility, band 2 was subjected to EM after negative staining. Fig. 3(a) shows a typical part of an electron micrograph containing monomeric CP43′–PSI complexes. A data set of 11 576 particles was extracted from the micrographs by selecting all the discernable particles and these were subjected to iterative rounds of multi-reference alignment and multivariate statistical classification in order to average similar images. Two different types of particle were present in the data set and are shown as averaged top views of the stromal surface in Fig. 3(b) and (c). With the aid of the published X-ray data for CP43 [15], we conclude that in the majority of complexes shown in Fig. 3(b), six CP43′ subunits form a crescent along one side of the monomer (Fig. 3(f)). This projection and modelling can be compared with the monomeric segment of the 18-mer CP43′–PSI supercomplex isolated from wild-type cells grown in minus iron (Fig. 3(d) and (e)) and reported previously [3–6]. This comparison aided the alignment of the X-ray data for the PSI monomer into the projection map of the 6-mer CP43′–PSI supercomplex of the PsaL$^-$ mutant. In this way, we conclude that the six CP43′ subunits are attached on the same surface in both cases; the surface where PsaJ and PsaF subunits are located. In the case of the slightly larger particles shown in Fig. 3(c), the modelling using X-ray data suggested that seven CP43′ subunits were present (Fig. 3(g)). This 7-mer complex was less abundant being <10% of the 6-mer supercomplex in the data set.

4. Discussion

We conclude that the CP43′ protein induced under iron deficiency in *Synechocystis* does not require the PSI reaction centre to be in a trimeric conformation for it to functionally couple and form a CP43′–PSI supercomplex. Moreover, this association of CP43′ with monomeric PSI is not dependent on the presence of PsaL. Electron microscopy and image processing of single particles in 'top' views coupled with comparison of projection maps from X-ray data indicate that six or seven CP43′ subunits associate with the PSI monomer. The 6-mer CP43′–PSI supercomplex seems to be very similar to the equivalent monomeric segment of the 18-mer CP43′–PSI supercomplex with its trimeric PSI reaction centre core. The presence of extra density along the exposed surfaces of the monomer compared to the non-exposed surfaces of the monomeric segment of the 18-mer CP43′–PSI supercomplex is due to the detergent shell, which has been estimated to be 10–15 Å [16]. The slightly larger particle apparently having seven CP43′ subunits suggests that increased exposure of the edge of the PSI reaction centre in the monomer compared to the trimer allows an additional CP43′ subunit to associate with it. In the case of the 18-mer CP43′–PSI supercomplex, it has been shown by steady-state fluorescence [3,4] and fluorescence and absorption spectroscopy [7,8] that energy transfer from the 18-mer CP43′ ring to the PSI reaction centre trimer is highly efficient. In the case of the 6 and 7-mer CP43′–PSI supercomplex reported here, there also seems to be good energy transfer since the CP43′ fluorescence at 685 nm is relatively low, but can be greatly enhanced by a mild triton treatment. The level of emission from CP43′, compared to that at 720 nm is, however, higher than that recorded with the intact 18-mer CP43′–PSI supercomplex [3]. This is probably due to more loosely asso-

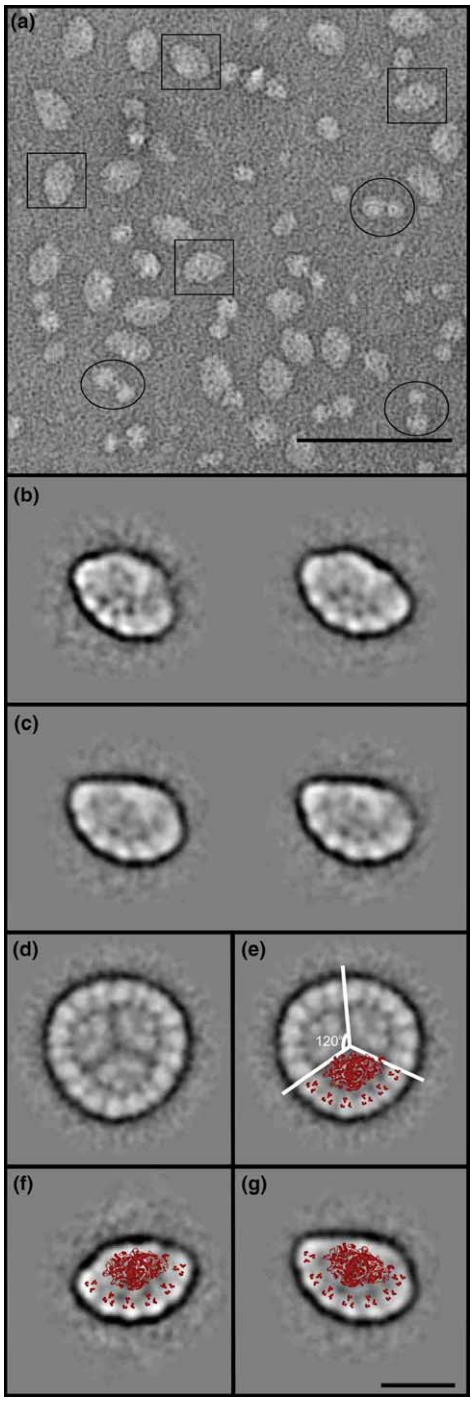

Fig. 3. (a) An electron micrograph containing purified CP43′–PSI monomeric complexes from *Synechocystis* sp. PCC 6803. Monomeric CP43′-PSI particles are boxed. Co-purifying ATP-synthase particles are ringed. Scale bar 800 Å: (b) shows class averages of CP43′–PSI complexes with 6 CP43′ subunits per PSI reaction centre. (c) shows class averages of CP43′–PSI complexes with 7 CP43′ subunits per PSI reaction centre. Projection maps shown in (b) and (c) result from the classification of the 11 576 single particle 'top' views of the stromal surface. (d) Top projections obtained by single particle analyses of wild type 18-mer CP43′–PSI supercomplex induced under iron stress. (e) Overlay of X-ray C_α-structure of PSI from Jordan et al. [2] and of CP43 from Ferreira et al. [15] onto one monomeric segment of the 18-mer CP43′–PSI supercomplex. (f) Overlay of X-ray C_α-structure of PSI [2] and CP43 [15] onto the 6-mer CP43′–PSI projection map shown in Fig. 3(b). (g) As (f) but for the 7-mer CP43′–PSI projection map shown in Fig. 3(c). Scale-bar for (b)–(g) 125 Å.

ciated CP43′ which is not functionally coupled with the 6-mer CP43′–PSI supercomplex, including the additional CP43′ subunit observed in some particles. In any event, the results presented here suggest that the stabilisation of the CP43′ antenna system in iron-starved cells of *Synechocystis* not only involves protein–protein interaction between adjacent CP43′ subunits but also between CP43′ and the monomeric PSI reaction centre.

We suggest that CP43′ organisation in the antenna ring is stabilised primarily by interactions between adjacent CP43′ subunits, with a localised specific interaction with each PSI monomer. This specific interaction is required to account for the preferential binding of CP43′ to one face of a monomeric PSI particle. Our hypothesis would imply that there is a specific subunit or region of PSI that is required for interaction with CP43′. Interestingly, Kouřil et al. [17] recently showed that, in a PsaFJ null mutant, CP43′ forms a 17-mer ring around the PSI trimer. This apparently contradicts our hypothesis, since with a 17-mer ring the PSI–CP43′ interaction cannot be same for each PSI monomer [17]. However, we suggest that in the PsaFJ mutant the 17-mer CP43′ ring may be anchored to the PSI trimer by a specific interaction with just one of the PSI monomers, with most of the CP43′ held in place by CP43′–CP43′ interaction and non-specific van der Waal's attraction to the surface of PSI.

Further structural studies and mutagenesis will be required to clarify the nature of the specific interaction between CP43′ and PSI. A 3D structure of the 18-mer CP43′–PSI supercomplex of *Synechocystis*, recently determined by cryo-EM in the absence of negative stain [5], confirmed that there is close interaction between the adjacent CP43′ subunits in the antenna ring. However, the lower density between the trimer surface and the surface of the CP43′ antenna rings suggests a weaker interaction. Nevertheless, the cryo-EM structure indicated a connecting density between a CP43′ and the PSI surface which could be due to the presence of a specific linker protein. This density is located in approximately the same position as the PsaG protein identified in a recent X-ray structure of the LHCI–PSI supercomplex of higher plants [18].

Plant PSI is monomeric and four light-harvesting chlorophyll-proteins (Lhca 1–4) bind along one side of the complex, which is equivalent to the outer face of the cyanobacterial PSI trimer [18]. The PsaG subunit may be responsible for specific interaction of Lhca with PSI [18]. Thus, the association of Lhca with PSI in plants is strikingly similar to the association of CP43′ with monomeric PSI in cyanobacteria. The cyanobacterial linker protein has yet to be identified.

Acknowledgements: J.B. and C.W.M. acknowledge financial support from the Biotechnology andBiological Science Research Council (BBSRC). J.D. and C.L.A. were recipients of EPSRC and BBSRC studentships, respectively.

References

[1] Chitnis, V.P. and Chitnis, P.R. (1993) FEBS Lett 336, 330–334.
[2] Jordan, P., Fromme, P., Witt, H.T., Klukas, O., Saenger, W. and Kraus, N. (2001) Nature 411, 909–916.
[3] Bibby, T.S., Nield, J. and Barber, J. (2001) Nature 412, 743–745.
[4] Bibby, T.S., Nield, J. and Barber, J. (2001) J. Biol. Chem. 276, 43246–43252.
[5] Nield, J., Morris, E.P., Bibby, T.S. and Barber, J. (2003) Biochemistry 42, 3180–3188.

[6] Boekema, E.J., Hiffney, A., Yakushevska, A.E., Piotrowski, M., Keegrstra, W., Berry, S., Michel, K.-P., Pisotorius, E.K. and Kruip, J. (2001) Nature 412, 745–748.
[7] Andrizhiyevskaya, E.G., Schwabe, T.M.E., Germano, M., D'Haene, S., Kruip, J., van Grondelle, R. and Dekker, J.P. (2002) Biochim. Biophys. Acta 1556, 265–272.
[8] Melkozernov, A.N., Lin, S., Bibby, T.S., Barber, J. and Blankenship, R.E. (2003) Biochemistry 42, 3893–3903.
[9] Viera, J. and Messing, J. (1982) Gene 19, 259–268.
[10] Vermaas, W.F.J., Charité, J. and Eggers, B. (1990) in: Current Research in Photosynthesis (Baltscheffsky, M., Ed.), Vol. 1, pp. 231–238, Kluwer Academic Publishers, Dordrecht.
[11] Hankamer, B., Nield, J., Zheleva, D., Boekema, E.J., Jansson, S. and Barber, J. (1997) Eur. J. Biochem. 243, 422–429.
[12] van Heel, M., Harauz, G. and Orlova, E.V. (1996) J. Struct. Biol. 116, 17–24.
[13] van Heel, M., Gowen, B., Matedeen, R., Orlova, E.V., Finn, R., Pape, T., Cohen, D., Stark, H., Schmidt, R., Schatz, M. and Partwardhan, A. (2000) Quart. Revs. Biophys. 33, 307–369.
[14] Sherman, M., Soejima, T., Shui, W. and van Heel, M. (1998) Ultramicroscopy 74, 179–199.
[15] Ferreira, K., Iverson, M., Maghlaoui, K., Barber, J. and Iwata, S. (2004) Science 303, 1831–1838.
[16] Guex, N. and Peitsch, M.C. (1997) Electrophoresis 18, 2714–2723.
[17] Kouřil, R., Yeremenko, N., D'Haene, S., Yakushevska, A.E., Keegstra, W., Matthijs, H.C.P., Dekker, J.P. and Boekema, E.J. (2003) Biochim. Biophys. Acta 1607, 1–4.
[18] Ben-Shem, A., Frolow, F. and Nelson, N. (2004) Nature 426, 630–635.